THE JOURNAL OF BIOLOGICAL CHEMISTRY VOL. 285, NO. 23, pp. 17614–17627, June 4, 2010

Bax Forms an Oligomer via Separate, Yet Interdependent, Surfaces*

Received for publication, February 11, 2010, and in revised form, April 1, 2010 Published, JBC Papers in Press, April 9, 2010, DOI 10.1074/jbc.M110.113456

Zhi Zhang[‡], Weijia Zhu[§], Suzanne M. Lapolla[‡], Yiwei Miao[¶], Yuanlong Shao[¶], Mina Falcone[§], Doug Boreham[‖], Nicole McFarlane[‖], Jingzhen Ding[‡], Arthur E. Johnson[¶‡‡], Xuejun C. Zhang[§§1], David W. Andrews[§2], and Jialing Lin[‡3]**

*From the [‡]Department of Biochemistry and Molecular Biology, University of Oklahoma Health Sciences Center, Oklahoma City, Oklahoma 73126, the Departments of [§]Biochemistry and Biomedical Sciences and [‖]Medical Physics and Applied Radiation Science, McMaster University, Hamilton, Ontario L8N 3Z5, Canada, the Departments of [¶]Molecular and Cellular Medicine, **Chemistry, and [‡‡]Biochemistry and Biophysics, Texas A&M University System Health Science Center, College Station, Texas 77843, and the [§§]Crystallography Research Program, Oklahoma Medical Research Foundation, Oklahoma City, Oklahoma 73104*

Interactions of Bcl-2 family proteins regulate permeability of the mitochondrial outer membrane and apoptosis. In particular, Bax forms an oligomer that permeabilizes the membrane. To map the interface of the Bax oligomer we used Triton X-100 as a membrane surrogate and performed site-specific photocross-linking. Bax-specific adducts were formed through photo-reactive probes at multiple sites that can be grouped into two surfaces. The first surface overlaps with the BH1–3 groove formed by Bcl-2 Homology motif 1, 2, and 3; the second surface is a rear pocket located on the opposite side of the protein from the BH1–3 groove. Further cross-linking experiments using Bax BH3 peptides and mutants demonstrated that the two surfaces interact with their counterparts in neighboring proteins to form two separated interfaces and that interaction at the BH1–3 groove primes the rear pocket for further interaction. Therefore, Bax oligomerization proceeds through a series of interactions that occur at separate, yet allosterically, coupled interfaces.

Mitochondrial outer membrane permeabilization (MOMP)[4] is the commitment step of apoptosis regulated by the proteins of Bcl-2 family (1–3). These proteins contain at least one of the four Bcl-2 homology (BH) motifs. Bax and Bak are required for MOMP and contain BH1, -2, and -3 motifs, although a BH4 motif was recently found in these proteins based on structural comparison with antiapoptotic family members (4). Bcl-2, Bcl-x_L, and other antiapoptotic members contain all four BH motifs and function to inhibit Bax/Bak-mediated MOMP. The other members of the Bcl-2 family, such as Bad and Bim, only contain a BH3 motif. Another common feature within the Bcl-2 family is a hydrophobic sequence located at the C terminus of some members. Structures of Bax and Bak have been revealed (5, 6). Both structures share a similar fold that contains a hydrophobic groove formed by BH1–3 regions (termed as BH1–3 groove hereafter). The structure of Bak, in which the BH1–3 groove is empty, was determined by using the soluble domain without the C-terminal hydrophobic sequence. In contrast, the BH1–3 groove in the structure of full-length Bax, as shown in Fig. 1*A*, is occupied by the C-terminal hydrophobic α-helix (α9). Unlike Bak that is constitutively anchored in the MOM by the C-terminal hydrophobic sequence, Bax is a monomeric protein in the cytosol and integrates into the MOM only after activation by BH3-only proteins or other factors (7–11). Active Bax and Bak in the MOM form oligomers that are required for MOMP (9, 12–13). To understand membrane permeabilization by Bax and Bak, it is important to characterize the interface between the proteins in the oligomers.

Following a treatment by truncated Bid (tBid) Bak oligomerizes in the MOM via two interfaces that were recently revealed (14, 15). The first interface is formed by reciprocal binding of the BH3 region to the BH1–3 groove of two Bak molecules (Fig. 1*B*, *front:front interface*); the second one involves two interacting α6 helices located on the opposite side of the protein from the first interface (Fig. 1*B*, *rear:rear interface*). In the absence of tBid or other apoptotic stimuli, Bak is integrated into the MOM via the C-terminal hydrophobic sequence with the N-terminal domain located in the cytosolic side of the MOM. It appears that, in the absence of an apoptotic signal, most Bak remains monomeric in the MOM, but some fraction can be bound by VDAC2 (voltage-dependent anion channel 2) or by an antiapoptotic family member such as Bcl-x_L that binds to the MOM after activation (16–18). The binding with Bcl-x_L is likely mediated by an interaction between the BH3 region of Bak and the BH1–3 groove of Bcl-x_L (19). During apoptosis Bad or another BH3-only protein may activate Bak by displacing Bak from the BH1–3 groove of Bcl-x_L without directly binding to Bak (16, 20, 21). The freed Bak can then oligomerize via the two interfaces described above.

* This work was supported, in whole or in part, by National Institutes of Health Grant GM062964 (to J. L.). This work was also supported by Canadian Institutes of Health Research Grant FRN 12517 (to D. W. A. and Brian Leber).

[1] Present address: Institute of Biophysics, Chinese Academy of Sciences, 15 Datun Rd., Beijing 100101, China.

[2] Holds the Tier 1 Canada Research Chair in Membrane Biogenesis.

[3] To whom correspondence should be addressed: 940 Stanton L. Young Blvd., Biomedical Sciences Bldg. 935, P. O. Box 26901, Oklahoma City, OK 73126-0901. Tel.: 405-271-2227 (ext. 61216); Fax: 405-271-3092; E-mail: jialing-lin@ouhsc.edu.

[4] The abbreviations used are: MOMP, mitochondrial outer membrane permeabilization; ϵANB-Lys, N^{ϵ}-(5-azido-2-nitrobenzoyl)-Lys; ANB, 5-azido-2-nitrobenzoyl; BH, Bcl-2 homology; CHAPS, 3-[(3-cholamidopropyl)dimethylammonio]-1-propanesulfonate; IRES, internal ribosome entry site; MOM, mitochondrial outer membrane; TM, transmembrane; TNFα, tumor necrosis factor α; WT, wild type; GFP, green fluorescent protein; tBid, truncated Bid.

Although Bax oligomerization can also be induced by tBid, the mechanism is likely different. Monomeric Bax is equilibrated between cytosolic soluble and peripheral MOM-bound states in healthy cells. Upon apoptotic stimulation tBid interacts with Bax exposing the targeting signals at both N- and C-terminal regions that localize Bax to mitochondria (11, 13, 22–26). Once at mitochondria Bax embeds its α9 as well as α5 and α6 helices into the MOM, which follows by oligomerization (27). Therefore, Bax activation may always require a direct interaction with BH3-only protein or some other activator protein, whereas such interaction may not always be required for Bak activation. This implies that the Bax oligomer may contain a BH3-only protein that may mask one of the two interacting surfaces similar to those revealed in Bak oligomer thereby inhibiting oligomerization. Thus, should Bax oligomerize in the same way as proposed for Bak, the BH3-only protein that activates Bax must be displaced (Fig. 1*B*). Alternatively, Bax may stay in the complex with the activating BH3-only protein but use different surfaces to oligomerize. There is also evidence in some systems that oligomerization of Bak may require a direct interaction with a BH3-only protein (28–30).

The possibility that one of the potential surfaces for Bax oligomerization interacts with a BH3-only protein is supported by a NMR structure in which a stabilized helical BH3 peptide from Bim binds Bax through a pocket that consists of α1, the loop connecting α1 and α2, and α6 (Fig. 1*A*, colored in *dark gray*) whose counterpart in Bak forms the rear:rear interface in the oligomer (31). Additional evidence for binding of a BH3-only protein to the rear pocket comes from a recent observation that a hemagglutinin-tagged α1 of Bax interacts with several BH3-only proteins, including Bim (28). However, this study also suggests that the BH1–3 groove may serve as the second binding pocket for the BH3-only protein because coprecipitation of tBid and Bax was abolished by a mutation in the pocket. Thus, should the activated Bax interact at both front and rear surfaces to form the two interface oligomer (Fig. 1*B*), the BH3-only activator must leave Bax prior to oligomerization. However, the one interface oligomer model in which the BH3-only protein remains bound to Bax oligomer cannot be ruled out, because binding of BH3-only protein to the rear pocket of Bax may induce a conformational change in Bax that would release α9 from the BH1–3 groove at the front side exposing the BH3 motif, which then could interact with the rear pocket of and activate the next Bax in the same way as the Bim BH3 peptide. In fact a Bax BH3 peptide can activate Bax, and the activated Bax can then activate another Bax through a mechanism termed auto-activation (32), a notion that was coined previously to describe a similar activation mechanism for Bak (33). Therefore, both auto-activation and oligomerization of Bax could be mediated by only one type of interface formed between the front and rear surfaces (Fig. 1*C*). The BH3-only protein that initially activates Bax may remain bound to the rear pocket of the first Bax in the oligomer or may be displaced only when the oligomer circulates.

To determine which model best describes Bax oligomerization, we employed a site-specific photocross-linking approach with single photoreactive probes located in both BH1–3 groove and rear pocket. Prior to cross-linking Triton X-100 micelles were added to induce Bax oligomerization similar to that seen when a BH3-only protein is added to Bax and the MOM. Unlike the conclusion from a recent study that Bax exists as monomer in the micelle (34), our data show that Bax forms an oligomer that contains two types of interface similar to those proposed for Bak oligomer. Because the rear pocket of Bax binds BH3-only protein during activation, our results indicate that the BH3-only protein must depart from the pocket before the activated Bax can oligomerize. We suggest that the interaction between two activated Bax proteins at the BH1–3 groove may be the trigger for the departure of the BH3-only protein. Moreover, the interaction mediated by the BH1–3 regions at the front:front interface primes the rear pocket to form the rear:rear interface. Therefore, our study reveals a mechanism by which Bax can form an oligomer through two interdependent surfaces.

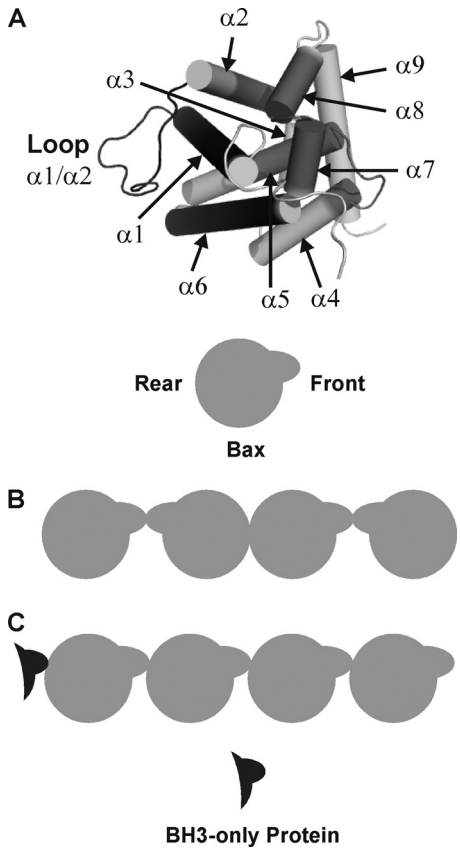

FIGURE 1. **Two competing models of Bax oligomerization.** *A*, structure of Bax monomer. The structure was drawn based on the coordinates 1F16 in the Protein Data Bank using PyMOL (DeLano Scientific). All α-helices and the loop between α1 and α2 are indicated. The front surface that includes BH1–3 regions is colored in *medium gray*. The rear surface formed by α1, the loop between α1 and α2, and α6 are colored in *dark gray*. The *schematic* underneath represents the Bax structure with front and rear surfaces. *B*, two-interface model. Bax oligomerizes through two different kinds of interface. One is formed by interaction of the front surfaces of neighboring molecules, and other by interaction of the rear surfaces. No BH3-only protein remains on Bax oligomer after it activates Bax. *C*, one-interface model. Bax oligomer contains only one type of interface that is formed by interaction of the front surface of a molecule and the rear surface of its neighbor. BH3-only protein that activates the first Bax in the oligomer may remain on its rear surface.

EXPERIMENTAL PROCEDURES

Plasmids, Proteins, and Peptides—To construct plasmids of Bax mutants for *in vitro* transcription and translation, we

used a plasmid that contains the coding region of full-length human Bax inserted between NcoI and EcoRI sites in the vector pSPUTK (Stratagene). Lys-null Bax mutant (K0) was generated by mutating all Lys codons in the Bax coding region to Arg codon. Bax mutants with a single Lys codon at a particular position were generated by mutating the corresponding codon of the K0 mutant to Lys codon and are designated here as "K" followed by a number that indicates the codon position. For example, the mutant Bax K73 has a single Lys codon at position 73 of the sequence. The codon for Gly^{67} in Bax K79 and K134 was changed to Arg codon to create the G67R mutants.

To construct plasmids of Bax mutants for testing the pro-apoptotic activity in cells, we used pBabe-MN-Bax-IRES-GFP plasmid (27). The NcoI site at 1226 bp of the plasmid was mutated to make the NcoI site at 8 bp unique. The NcoI-StuI fragment of the Bax coding region in the mutated plasmid was replaced by that from the pSPUTK-Bax K0 plasmid to generate pBabe-MN-Bax K0-IRES-GFP plasmid. Then, the NcoI-BamHI fragment of pBabe-MN-Bax K0-IRES-GFP plasmid was replaced by that from pSPUTK-Bax single K mutant plasmid to generate the corresponding pBabe-MN-Bax single K mutant-IRES-GFP plasmid.

The plasmid for expression a His_6-tagged Bax in *Escherichia coli* was modified from the pTYB1-Bax plasmid (5) by inserting a coding sequence for MH_6GENLYFQGT prior to the Bax coding sequence. The codon for Gly^{67} of Bax in the plasmid was changed to Arg codon to create the G67R mutant. All of the Bax mutant plasmids were generated by using appropriate primers and the overlapping PCR-based method (35) or the QuikChange method (Stratagene), and verified by DNA sequencing.

Expression and purification of His_6-tagged human Bcl-2 lacking the transmembrane (TM) sequence (His_6-Bcl-2ΔTM), and the mutant with Gly^{145} replaced by Ala (His_6-Bcl-2ΔTM-G145A) proteins were done as described previously (36). Expression and purification of His_6-tagged Bax was done as described (37), except that the His_6-Bax protein eluted from the chitin column was dialyzed to remove 2,2′,2′′,2′′′-(ethane-1,2-diyldinitrilo)tetraacetic acid and then purified using a Ni^{2+}-nitrilotriacetic acid-agarose column. The purified protein was dialyzed in buffer A (100 mM NaCl, 20% (v/v) glycerol, and 10 mM HEPES, pH 7.5). The peptides containing α-helix 2 (H2), α-helices 2 and 3 (H2 and H3) of human Bax, and their G67R mutants were synthesized as described before (32).

Proapoptotic Activity of Bax Mutants in Cells—HEK293 cells were transfected with a plasmid encoding the eco receptor to generate a cell line that can be infected with murine retrovirus. Replication-incompetent murine retroviruses that contain the pBabe-MN-Bax mutant-IRES-GFP plasmid described above and hence coexpress the Bax mutant and green fluorescent protein (GFP) were prepared using Phoenix cells as a packaging line, and the amount of virus was determined using real-time PCR. This is necessary as the more pro-apoptotic a Bax mutant is the less virus the packaging cells make before they die. Furthermore, viruses expressing a pro-apoptotic protein do not form plaques. Equal numbers of virus were used to infect the HEK293 human embryonic kidney cells for 48 h (infection efficiency was ~20%). One of duplicate sets of the cells was stained with Annexin V, whereas the other set was treated with tumor necrosis factor α (TNFα) and cycloheximide for 6 h and then stained with Annexin V. The fraction of Annexin V-positive cells was determined for green cells (infected) and non-green cells (uninfected). This process underestimates the total amount of cell death, because only adherent cells are counted and at a single time point (not cumulative). Furthermore, cells that were not scored as green may express small amounts of Bax (and GFP) and therefore have increased Annexin V staining compared with cells infected with virus that expressed only GFP. Nevertheless, the assay can clearly reveal the proapoptotic activity of the Bax mutants relative to the wild-type Bax that was assayed in parallel.

Photocross-linking and Characterization of Photoadducts—[^{35}S]Met- and/or N^{ϵ}-(5-azido-2-nitrobenzoyl)-Lys (εANB-Lys)-labeled Bax proteins were translated *in vitro* from the corresponding RNAs as described (36, 38). Purified His_6-Bax (2 μM), His_6-Bax-G67R (2 μM), His_6-Bcl-2ΔTM (4 μM), and/or His_6-Bcl-2ΔTM-G145A protein (4 μM) was added to 10 μl of *in vitro* translated [^{35}S]Met/ANB-labeled single K Bax or the G67R mutant, and if indicated, 0.25% (v/v) of Triton X-100 was added. Photocross-linking, purification of the photoadduct using Ni^{2+}-nitrilotriacetic acid-agarose, and characterization of the photoadduct by SDS-PAGE and phosphorimaging were as described (36), except that an Amersham Biosciences Storm 840 PhosphorImager or a Fuji FLA-9000 image scanner was used for the phosphorimaging analysis. For photocross-linking with Bax peptide, 15 μM of H2, H2–H3, or the G67R mutant were added to 10 μl of *in vitro* translated [^{35}S]Met/ANB-labeled single K Bax, and the sample was processed as above, but skipping the Ni^{2+}-purification step.

Gel-filtration Chromatography to Assay Bax Oligomerization Induced by Triton X-100—Purified His_6-tagged Bax (2.2 μM) and/or Bcl-2ΔTM (2.2, 4.4, or 6.6 μM) or Bcl-2ΔTM-G145A (6.6 μM) protein was incubated in 25 μl of buffer A containing 0.25% (v/v) Triton X-100 at 4 °C for 1 h. The sample was adjusted to 300 μl with buffer B (300 mM NaCl, 0.2 mM dithiothreitol, 2% (w/v) CHAPS, and 20 mM HEPES, pH 7.5) and then mixed with 50 μl of Ni^{2+}-nitrilotriacetic acid-agarose (50% (v/v) suspension in buffer B). After rocking at 4 °C for 2 h the Ni^{2+}-resin-bound proteins were washed twice with 1 ml of buffer B to remove Triton X-100, judged by reduction of the A_{280} to a baseline level (39). Then the proteins were eluted with 120 μl of buffer B containing 250 mM imidazole. The eluted proteins (100 μl) were injected into Superdex 200 HR10/30 column in AKTA-FPLC (Amersham Biosciences). The chromatography was developed in buffer B at a flow rate of 0.4 ml/min, and fractions of 500 μl were collected. The fractions were precipitated with Cl_3CCOOH and analyzed by 15% SDS-PAGE, immunoblotting with a Bax- or Bcl-2-specific antibody, and the corresponding proteins were detected with enhanced chemiluminescence.

For the reaction containing purified His_6-Bax protein and *in vitro* translated [^{35}S]Met-Bax protein, 2.2 μM His_6-Bax and 0.25% Triton X-100 were added to 100 μl of [^{35}S]Met-Bax, and the sample (~140 μl) was incubated at 4 °C for 1 h. The sample was then adjusted to 350 μl with buffer B, and mixed with 100 μl of the Ni^{2+}-resin suspension. The sample was processed as

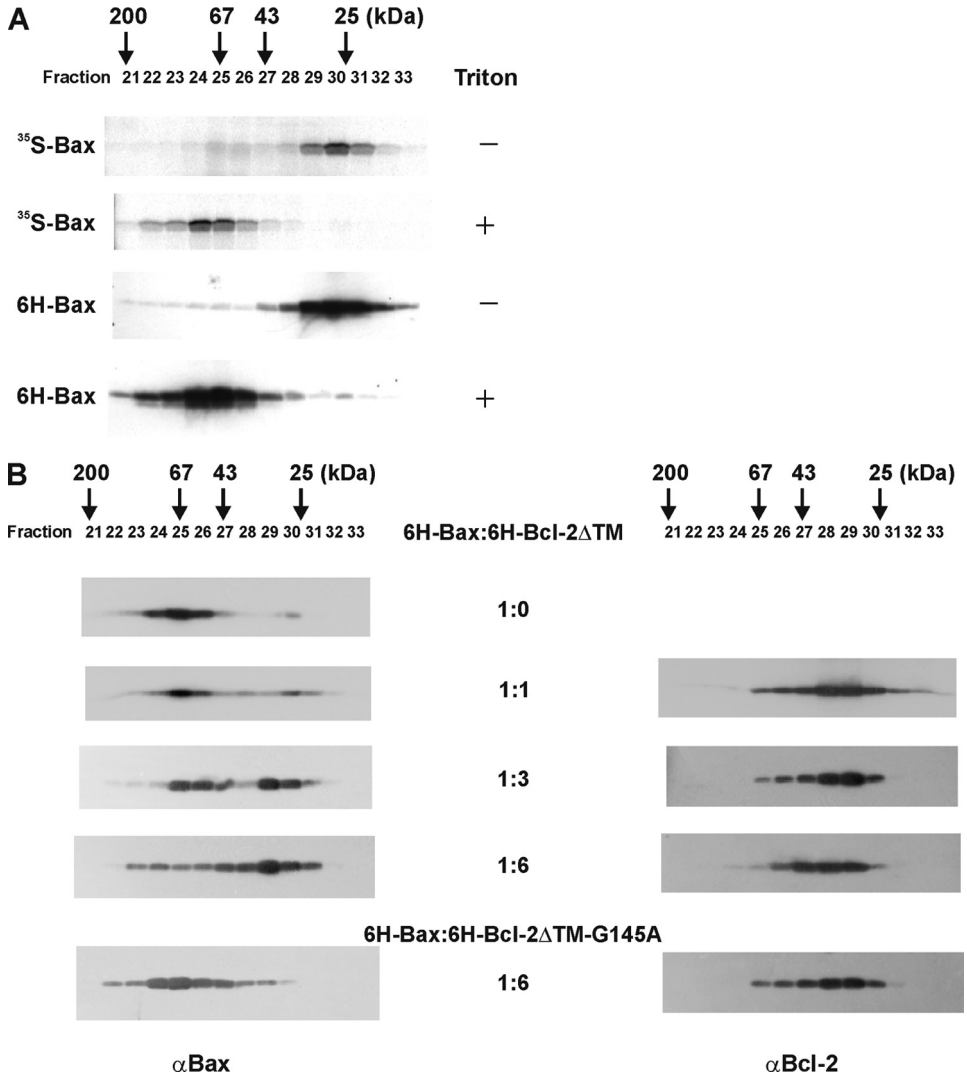

FIGURE 2. **Oligomerization of Bax induced by Triton X-100 and inhibited by Bcl-2.** *A*, oligomerization of *in vitro* synthesized [^{35}S]Met-labeled Bax (*^{35}S-Bax*) and purified His$_6$-tagged Bax (*6H-Bax*) proteins in the absence and presence of Triton X-100 examined by gel-filtration chromatography. The chromatographic *fractions 21–33* were analyzed by SDS-PAGE and phosphorimaging or immunoblotting with a Bax-specific antibody to detect [^{35}S]Met-Bax (*top two panels*) or 6H-Bax (*bottom two panels*), respectively. *B*, oligomerization of Triton X-100-treated His$_6$-Bax in the absence or presence of His$_6$-tagged Bcl-2ΔTM or Bcl-2ΔTM-G145A examined by gel-filtration chromatography. The chromatographic *fractions 21–33* were analyzed by SDS-PAGE and immunoblotting with a Bax- or Bcl-2-specific antibody to detect His$_6$-tagged Bax (*left panels*) or Bcl-2 (*right panels*). The molar ratios of Bax *versus* Bcl-2 or Bcl-2-G145A in the samples are indicated in the *middle*. In all *panels*, the elution positions for protein standards are indicated on the *top* with molecular mass.

described above. Then one-fourth of the Cl_3CCOOH-precipitated sample was analyzed by the SDS-PAGE and immunoblotting to detect His$_6$-Bax, and three-fourths of the sample was analyzed by the SDS-PAGE and phosphorimaging to detect [^{35}S]Met-Bax. For the His$_6$-Bax and [^{35}S]Met-Bax incubated in the absence of Triton X-100, the sample was processed in parallel as the proteins incubated in the presence of Triton X-100, except that the steps to remove Triton X-100 were omitted.

RESULTS

Bax Oligomerization Induced by Detergent—To determine the binding site on Bax for oligomerization using site-specific photocross-linking as described (36), we need to prepare one polypeptide containing a photoreactive cross-linking probe and the other a unique tag to permit isolation of the photoadduct. This method requires one Bax protein to be synthesized by *in vitro* translation to incorporate the photoreactive probe at a specific site, and [^{35}S]Met as a tracer. The binding partner is a purified recombinant Bax protein containing a His$_6$ tag at the N terminus that can be used to enrich the radioactive photoadduct using Ni^{2+}-chelating resin. Ideally oligomerization of these Bax proteins should be studied in the MOM. However, the yield of oligomers was not enough for the cross-linking study. We thus chose to study the Bax oligomer formed in detergent micelle as a membrane surrogate.

Non-ionic detergent, Triton X-100, was known to induce Bax conformational change and homo-oligomerization in cell lysate (8, 40). The detergent treatment also activated recombinant Bax to permeabilize liposomes and mitochondria (41). To determine whether the *in vitro* synthesized [^{35}S]Met-Bax and the purified His$_6$-Bax behave like the Bax in cell lysate that only forms oligomer in the presence of detergent, these proteins were first incubated in the absence of detergent. The resulting sample was treated with a zwitterionic detergent CHAPS at the concentration of 2% that is >0.6%, the critical micelle concentration, and subjected to gel-filtration chromatography. CHAPS was included in these steps to make the sample composition similar to the samples incubated in the presence of Triton X-100 (see below), and CHAPS does not change the oligomeric state of Bax (8, 40, 42). The eluted fractions were analyzed by SDS-PAGE and either phosphorimaging to detect the [^{35}S]Met-Bax or immunoblotting with a Bax-specific antibody to detect the His$_6$-Bax. As shown in Fig. 2*A*, both Bax proteins were eluted mainly before a protein marker with relative molecular mass of 25 kDa. Because the molecular mass predicted for each Bax protein (~21 kDa) in a micelle with 4–14 CHAPS molecules (average size of a CHAPS micelle, ~6 kDa) is ~27 kDa (43), these results suggest that both proteins are monomeric in the absence of Triton X-100.

Next, the [^{35}S]Met-Bax and His$_6$-Bax were coincubated in the presence of Triton X-100 at the concentration of 0.25% that is >0.05%, the critical micelle concentration. The resulting sample was bound to Ni^{2+}-resin to enrich the oligomer formed by the His$_6$-Bax and [^{35}S]Met-Bax. The bound fractions were

washed extensively with 2% CHAPS to remove Triton X-100. This is necessary because a Triton X-100 micelle contains 100–155 Triton X-100 molecules on average with molecular mass ~80 kDa (43), equivalent to a Bax tetramer, thereby preventing the use of gel-filtration chromatography to analyze Bax oligomerization. The bound fraction with Triton X-100 exchanged by CHAPS was then eluted by imidazole and subjected to the gel-filtration chromatography. Fractions eluted from the column were analyzed as described above. As shown in Fig. 2*A*, both Bax proteins were eluted as oligomers in CHAPS micelles, mainly trimer (~69 kDa) but large oligomers up to 200 kDa were also visible. Therefore, the gel-filtration data demonstrated that the interaction between the *in vitro* synthesized Bax and the recombinant Bax can be induced by Triton X-100 treatment resulting in a large extent of oligomerization similar to endogenous Bax.

Bax Oligomerization Inhibited by Bcl-2—It has been well established that Bcl-2 inhibits Bax oligomerization in biological systems (44). To determine whether Bcl-2 can inhibit Bax oligomerization in Triton X-100, the His_6-Bcl-2ΔTM was incubated with the His_6-Bax protein in 0.25% Triton X-100. Triton X-100 in the sample was exchanged for CHAPS prior to the gel-filtration chromatography as described above. Fractions from the gel-filtration chromatography were analyzed by SDS-PAGE and immunoblotting with an antibody specific to Bax or Bcl-2. As shown in the *left panel* of Fig. 2*B*, Bax protein shifted from the trimeric and large oligomeric factions to the dimeric and monomeric fractions in the presence of the Bcl-2 (Fig. 2*B*, *right panel*). Furthermore, more Bax proteins were seen in the dimeric and monomeric fractions as the concentration of Bcl-2 was increased. Therefore, Bcl-2 inhibits Triton X-100-induced Bax oligomerization in a dose-dependent manner. Of note, the Bcl-2 signal in the immunoblots does not correlate with the amount of Bcl-2 used in the experiments. Due to the limited linear range of immunoblotting it was necessary to load smaller amounts of the fractions from experiments with more Bcl-2 to ensure that the resulting blots remained in the linear range for comparison across the fractions. The amount of protein lost during the gel filtration is small and the same among the experiments as reflected by the similarity in total intensity for the blots shown.

To determine whether the inhibitory effect of Bcl-2 on Bax oligomerization is dependent on the interaction between Bcl-2 and Bax, we used His_6-Bcl-2ΔTM-G145A, a Bcl-2 mutant protein that does not interact with Bax (36, 45). As shown in the *bottom panel* of Fig. 2*B*, the mutant Bcl-2 does not inhibit Bax oligomerization, even at the highest Bcl-2 to Bax ratio, demonstrating that the Bcl-2 inhibition of Bax oligomerization requires the Bcl-2-Bax interaction. This result also indicates that the generation of monomeric Bax in the presence of Bcl-2 is due to the Bcl-2-Bax interaction. However, the resulting Bcl-2-Bax complex seems not stable, because Bax was eluted mainly as monomers in the presence of the highest concentration of Bcl-2. This may be due to CHAPS in the buffers, which has previously been shown to dissociate tBid-Bax complex and therefore may also dissociate the Bcl-2-Bax complex albeit less efficiently (18). Consistent with this possibility Bcl-2 was also eluted mainly as monomer (~25 kDa) in CHAPS micelles (~6 kDa) (Fig. 2*B*, *right panel*). Nevertheless, because the G145A mutation also abolishes the interaction of Bcl-2 with Bax and anti-Bax activity in cells (44, 45), our results suggest a biological relevance for the interaction between these proteins in Triton X-100.

Strategy to Capture Bax Homodimer by Site-specific Photocross-linking—To determine if the detergent-induced Bax homo-interaction can be captured by photocross-linking, we translated RNA encoding Bax *in vitro* in the presence of [^{35}S]Met and a modified lysyl-tRNA with an ANB moiety covalently attached to the ϵ-amino group of the lysine. The ϵANB-Lys-$tRNA^{Lys}$ is a functional aminoacyl-tRNA analog that recognizes the Lys codon in Bax RNA and incorporates the photoreactive Lys analog into the Bax protein (46). The ANB-labeled Bax protein was then incubated with the purified His_6-Bax protein in the presence of Triton X-100 to induce their interaction. Excess His_6-Bax was added to prevent the ANB-Bax from homo-interaction thereby increasing the yield of photoadduct between the ANB- and His_6-labeled proteins. Upon exposing the sample to UV light, a nitrene was generated from the ANB moiety, which is a powerful electrophile that rapidly reacts with any nearby heteroatoms possessing non-bonding electron pairs, double bond, or even C–H bond, including such heteroatoms or bonds in the bound His_6-Bax. The photolysis thus generated a photoadduct of covalently linked [^{35}S]Met-Bax and His_6-Bax that was then enriched by Ni^{2+}-resin, separated from other proteins by SDS-PAGE, and detected by phosphor-imaging.

Human Bax contains nine lysines and hence has the potential to be labeled by ANB at multiple sites. If one or more of these sites are close to or within the surface of [^{35}S]Met-Bax that contacts His_6-Bax, photoadducts can be formed between the two proteins. However, the precise locations of the photoreactive probe would be difficult to determine, and residues other than the lysines that are located in the binding surface would not be seen. To use the photocross-linking approach to map the binding surface, we generated a series of Bax mutants, each with a single Lys located at a specific location where the photoreactive probe will be incorporated. Each single Lys Bax mutant has a Lys substituting for a specific residue in a Lys-null Bax (Bax K0) that was constructed by replacing all of the lysines in wild-type Bax (Bax WT) with Arg (Fig. 3*A*).

The following criteria were employed to design the single Lys Bax mutants. 1) Only surface residues were replaced by Lys to avoid disrupting the protein core. 2) Conserved substitutions were preferred, wherever suitable, to minimize the impact on the protein surface. Of note, some of the lysines in Bax WT were kept individually to create several single Lys mutants. 3) Representative Bax mutants with a single Lys in some of the structurally important motifs were assayed in HEK293 cells for pro-apoptotic activity alongside Bax WT and Bax K0.

In the assay GFP was coexpressed with the Bax proteins from an internal ribosome entry site (IRES) in the same messenger RNA to identify cells expressing exogenous Bax. Annexin V labeling and GFP expression were measured by flow cytometry and used to compare the extent of apoptosis in retrovirus infected (GFP-positive) and non-infected (GFP-negative) cells. The *histograms* in Fig. 3*B* show the fraction of non-infected

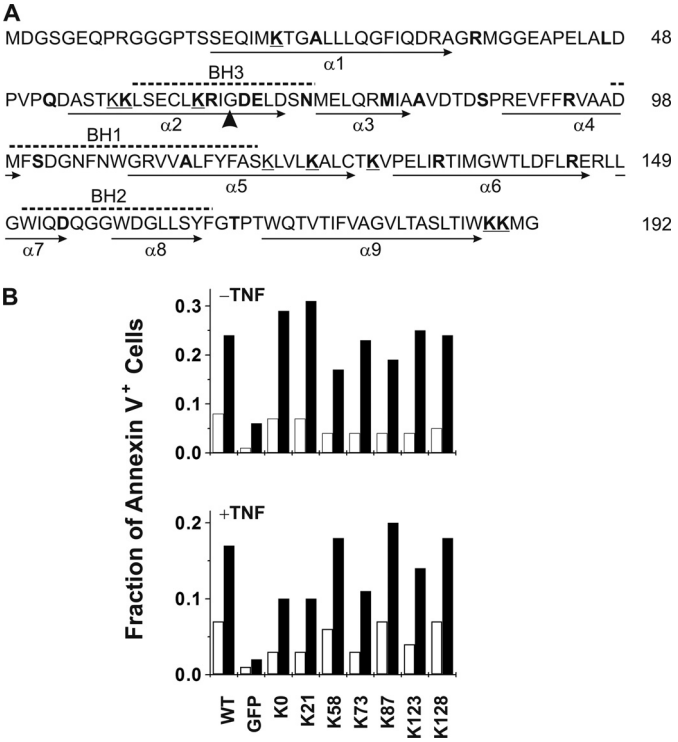

FIGURE 3. **Sequence and proapoptotic activity of Bax mutants.** *A*, Bax sequence is shown with BH motifs highlighted by *dashed lines* above and α-helices identified by *arrows* below. All nine lysines (*underlined Ks*) were changed to Arg to create Bax K0. Single Lys Bax mutants were created by replacing each of the residues highlighted in *bold* with a Lys. The *arrowhead* indicates Gly^{67} that was changed to Arg in the G67R mutant. *B*, activity of wild-type and mutant Bax proteins in HEK293 cells. The cells infected with retrovirus that coexpressed Bax and GFP from the same message using an IRES sequence between the two coding regions were examined for cell death 48 h after infection (*upper panel*) or after being treated with TNFα and cycloheximide for another 6 h. Both sets of cells were stained with Annexin V. *Upper panel*, untreated (*−TNF*), and *lower panel*, TNFα/cycloheximide-treated sample (*+TNF*), show the fraction of adherent Annexin V-positive cells in GFP-positive (Bax expressing) population (*black bar*) and the fraction of Annexin V-positive cells in GFP-negative population (not expressing or expressing only small amounts of Bax) (*white bar*). The type of Bax protein expressed by the virus that was used to infect the cells is indicated below the plot. GFP indicates the control virus that expressed only GFP, and WT, K0, or K21 etc. indicate the virus that expresses GFP and wild-type, Lys-null, or single Lys Bax, respectively. Data shown are from a representative experiment of three independent replicates.

cells (*white bars*) compared with the fraction of infected cells (*black bars*) that stained with Annexin V in the exact same well of the microtiter plate. Assume that Bax expression correlates with GFP expression from the IRES, the results clearly show that expression of Bax increased apoptosis in the cells. Furthermore, the increase of apoptosis was due to expression of exogenous Bax, because less apoptosis was detected in the cells that were either not infected or infected with the control retrovirus that expressed only GFP. This single time point assay does not measure cumulative cell death and underestimates the difference between "uninfected" and infected cells, because the threshold GFP expression used to separate the populations was arbitrary, and it is likely that some cells expressing low amounts of Bax and GFP were scored as uninfected. Even with these caveats the bias introduced should result in a similar underestimation of the proapoptotic activity for WT-Bax and the mutants. Importantly, there was a similar increase in Annexin V staining in the cells expressing WT Bax compared with the cells expressing the Bax mutants (Fig. 3*B*, *upper panel*). Thus expression of both WT Bax and the Bax mutants induced a similar extent of apoptosis in otherwise untreated cells. The cell death in these populations is mediated by the response of cells to expression of the exogenous Bax and the stress of being grown in culture. When these cells were treated with TNFα, there was an increase in Annexin V labeling that was further exacerbated by expressing either WT Bax or the mutant Bax (Fig. 3*B*, *lower panel*). These data suggest that the expression of Bax and the Bax mutants facilitated TNFα-induced apoptosis similarly. By considering all the data together we conclude that, when expressed in cells, the Bax mutants are approximately as proapoptotic as WT Bax.

Bax Homodimerization Can Be Detected by Site-specific Photocross-linking—To determine whether the homodimerization of Bax could be detected using site-specific photocross-linking we used Bax K73, a functional mutant with a single Lys replacing Asn^{73}, the last residue of the BH3 region (Fig. 3). The BH3 region is well known to play an important role in Bax homo-interaction (20, 47–49). The Bax mutant was synthesized by *in vitro* translation to incorporate [^{35}S]Met and an ANB-Lys at position 73. The resulting protein was incubated with His_6-Bax in the presence of Triton X-100. After photolysis, a product with an apparent molecular mass close to that predicted for the Bax dimer was detected (Fig. 4*A*, *lane 2*, indicated by *arrow*). The product is a photoadduct, because it did not form in the control experiment when ϵANB-Lys-$tRNA^{Lys}$ or UV irradiation was omitted (Fig. 4*A*, *lanes 1* and *3*). The product contains both [^{35}S]Met- and His_6-Bax because it is radioactive and bound to Ni^{2+}-resin, and was not formed in the absence of His_6-Bax (Fig. 4*A*, *lane 4*). Therefore, the product is the photoadduct formed by [^{35}S]Met-Bax and His_6-Bax. Of note, there was no [^{35}S]Met-Bax detected in the Ni^{2+}-bound fraction when His_6-Bax was not added to the sample (Fig. 4*A*, *lane 4*, indicated by the *circle*), demonstrating that detection of [^{35}S]Met-Bax in Ni^{2+}-bound fraction in the other samples (Fig. 4*A*, *lanes 1–3*) is due to its binding to His_6-Bax. The same explanation applies to other data shown in the other *lanes* of Figs. 4 and 5, because they were also obtained from the Ni^{2+}-bound fraction, but not to the data shown below in Fig. 7*C* that were from the total photocross-linking sample.

As expected when RNA encoding the Bax K0 control was translated, ANB-Lys was not incorporated into the Bax protein, because there is no Lys codon in the RNA. Although the [^{35}S]Met-Bax K0 protein still bound to the His_6-tagged Bax, and was therefore recovered from the Ni^{2+}-bound fraction (Fig. 4*A*, *lanes 5–7*, indicated by the *open circle*), no photoadduct was generated, as expected. The product indicated by the *closed circle* is not a photoadduct, because it was also formed in the absence of the ANB and UV irradiation. Therefore, the photoadduct formed by [^{35}S]Met-Bax K73 and His_6-tagged Bax was via the ANB probe attached to Lys^{73}. The photoadduct formation is due to position 73 being close to the interface of Bax homodimer, because the ANB probe at Lys^{73} of one Bax molecule was able to react specifically with micromolar concentrations of the His_6-tagged Bax molecule in the presence of high concentrations of reticulocyte proteins from the *in vitro* translation system, including ~150 mM globin. Moreover, the cross-

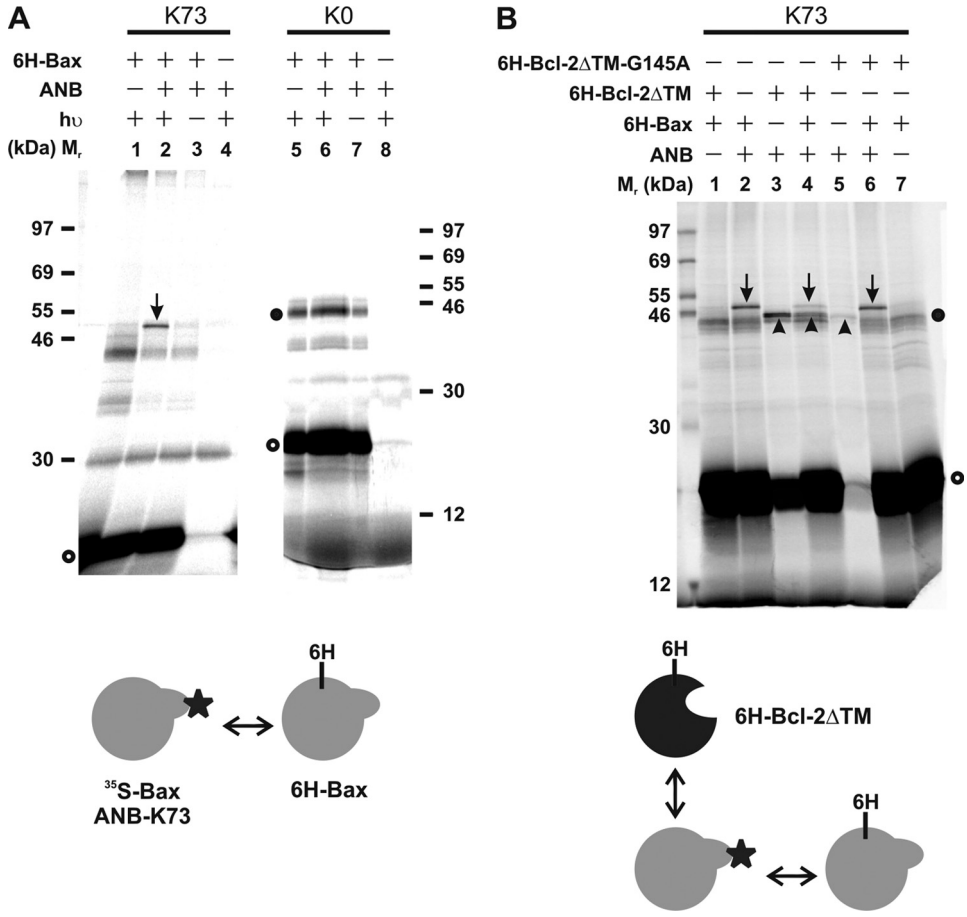

FIGURE 4. **Site-specific photocross-linking detected Bax dimerization in Triton X-100.** *A*, photocross-linking of His_6-tagged Bax to *in vitro* synthesized [^{35}S]Met-labeled Bax with a single ANB probe attached to K73 (*lanes 1–4*). The *schematic* underneath illustrates interaction between the two proteins (indicated by the *double-headed arrow*), in which the *star* attached to the front surface of [^{35}S]Met-Bax indicates the ANB probe. After photolysis the fractions that bound to Ni^{2+}-resin were analyzed by SDS-PAGE and phosphorimaging. A photoadduct was detected between the Bax K73 and His_6-Bax in *lane 2* and is indicated by an *arrow*. The adduct was absent when *in vitro* synthesized Bax K0 instead of Bax K73 was used (*lanes 5–8*). The *filled circle* adjacent to *lane 5* indicates a non-photoadduct formed by [^{35}S]Met-Bax K0. The *open circle* indicates the [^{35}S]Met-labeled Bax K73 or K0 monomer. Protein standards are indicated on the side of each phosphor image with molecular mass. *B*, inhibition of photocross-linking of the [^{35}S]Met/ANB-labeled Bax K73 to His_6-tagged Bax by His_6-tagged Bcl-2ΔTM (*lanes 1–4*) but not by Bcl-2ΔTM-G145A (*lanes 5–7*). The *arrow* indicates the photoadduct of [^{35}S]Met-Bax and His_6-Bax, and the *arrowhead* is the photoadduct of [^{35}S]Met-Bax and His_6-Bcl-2ΔTM or the G145A mutant. These photoadducts are specific to the corresponding protein pairs as they were not detected when one of the proteins (*lanes 2* and *3*), ϵANB-Lys-tRNA^{Lys} (*lanes 1* and *7*), or UV irradiation (data not shown) was omitted. The *schematic* underneath illustrates that His_6-tagged Bax, and His_6-tagged Bcl-2ΔTM compete for interaction with [^{35}S]Met- and ANB-labeled Bax. Other *symbols* are as described in *panel A*.

linking occurred via the Lys^{73}-ANB-derived reactive nitrene that has a relatively short lifetime of nanoseconds.

To check whether the site-specific photocross-linking captured a biologically relevant Bax dimer complex, we added His_6-Bcl-2ΔTM or its G145A mutant to the reaction. As shown in Fig. 4*B*, the formation of [^{35}S]Met-Bax/His_6-Bax photoadduct was reduced in the presence of His_6-Bcl-2ΔTM (compare the *arrow*-indicated bands in *lanes 2* and *4*). The presence of the Bcl-2 protein generated a new product (indicated by the *arrowhead* in *lane 4*), which is a [^{35}S]Met-Bax/His_6-Bcl-2ΔTM photoadduct, because it is the only photoadduct formed when only His_6-Bcl-2ΔTM was added to the photoreaction (indicated by the *arrowhead* in *lane 3*). The presence of His_6-Bax also reduced the amount of [^{35}S]Met-Bax/His_6-Bcl-2ΔTM photoadduct (compare the *arrowhead*-indicated bands in *lanes 3* and *4*). In contrast, very little Bax/Bcl-2 photoadduct was formed when the His_6-Bcl-2ΔTM-G145A was used (indicated by the *arrowhead* in *lane 5*), and as expected the mutant did not inhibit the formation of Bax homo-photoadduct (compare the *arrow*-indicated bands in *lanes 2* and *6*). These findings are consistent with the competitive nature of Bax homo- and hetero-interaction with Bcl-2 observed in biological systems, which relies on the interaction between the two proteins and is prevented by the G145A mutation (45, 47, 50). Further evidence that the G145A mutation inhibits the Bcl-2 interaction with Bax can be found by comparing the *circle*-indicated [^{35}S]Met-Bax monomer band in *lane 5* with other *lanes* in Fig. 5*B*. Clearly there is almost no [^{35}S]Met-Bax detected in *lane 5*, which indicates that the radioactive protein did not bind to the His_6-tagged G145A Bcl-2 mutant. These data also indicate that the Bax synthesized by *in vitro* translation behaved similarly to Bax expressed in cells as it bound to WT Bcl-2 but not the G145A mutant. As mentioned above, Bax synthesized *in vitro* also bound His_6-tagged Bax (Fig. 4*A*), which is another indication that the protein is active. Finally a mutation that inhibited the function of Bax in cells also inhibited the binding between these Bax proteins (see Fig. 8), consistent with the notion that our system reconstitutes authentic binding interactions between the proteins.

Interface of Bax Homo-oligomer Revealed by Site-specific Photocross-linking—Because photocross-linking of Bax with an ANB-Lys located at position 73 with His_6-Bax indicates the proximity of this position to an interface of the two molecules in the complex, other sites of contact or close approach for the molecules in the complex can be similarly mapped by altering the location of the photoreactive Lys. We therefore prepared 23 additional Bax mutants, each with a single ANB-Lys located at a specific location, and performed the photocross-linking reaction. The results shown in Fig. 5 indicate that the following residues are close to the interface of the neighboring proteins in the Bax complex: 24 in helix 1, 37, and 47 in the loop between helices 1 and 2 (termed loop 1), 68 and 69 in helix 2, 73 in loop 2 (data shown in Fig. 4*A*), 79 in helix 3, 82 in loop 3, and 134 and 145 in helix 6. In addition, residue 189 and/or 190 near the C terminus is close to the interface as indicated by the data from Bax K189,190.

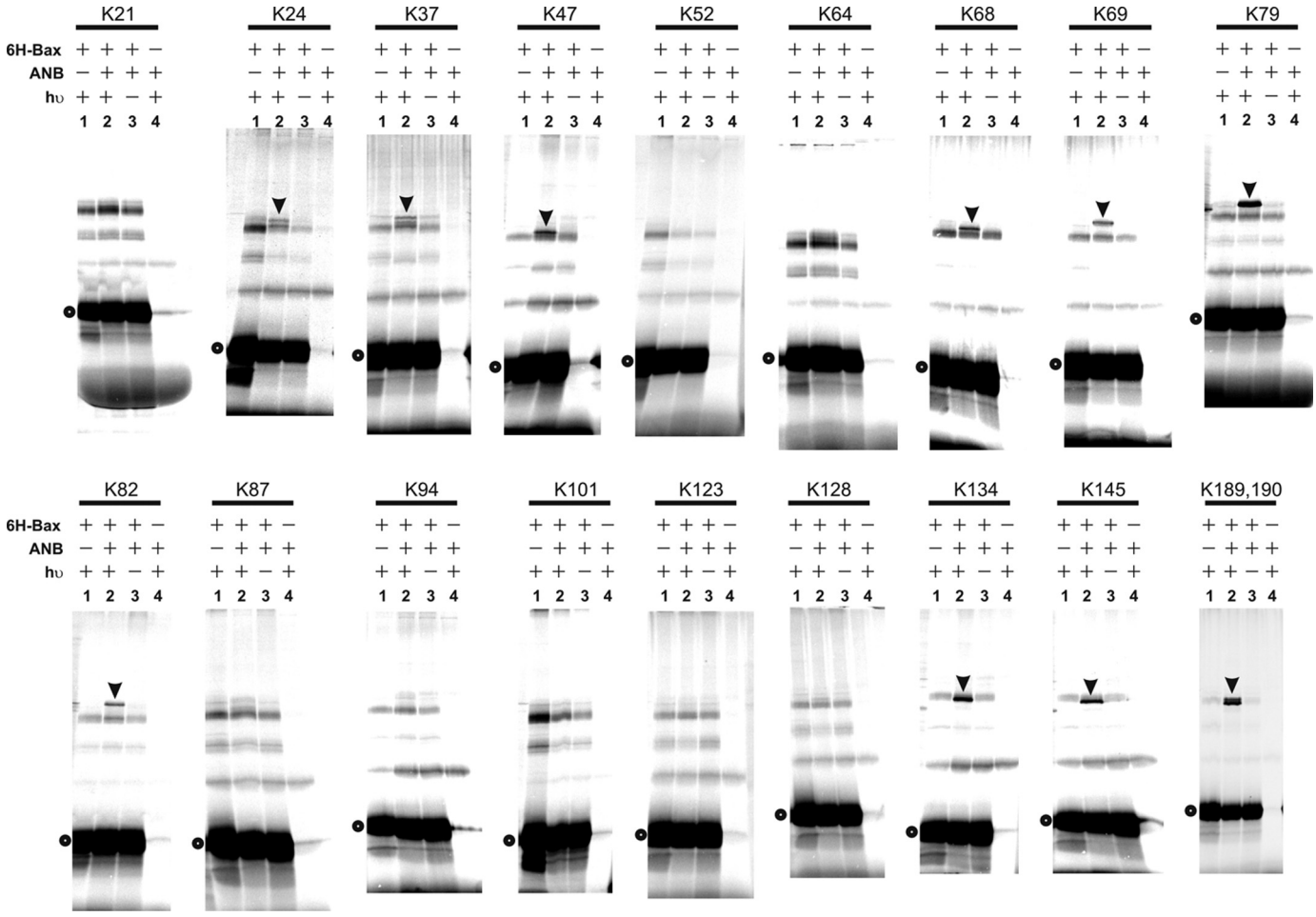

FIGURE 5. **Photocross-linking of His_6-tagged Bax protein to [^{35}S]Met-labeled Bax proteins, each with a single ANB-labeled Lys residue.** The Ni^{2+}-resin-bound photolyzed samples were analyzed as above. The position of the single lysine in [^{35}S]Met-Bax protein is indicated at the *top* of each *image*. The [^{35}S]Met-Bax/His_6-Bax-specific photoadduct and the [^{35}S]Met-Bax monomer that was bound to the Ni^{2+}-resin via interaction with His_6-Bax are indicated by an *arrowhead* and *open circle*, respectively. For simplicity the molecular mass standards are not shown, although they were included in all SDS-PAGE analyses.

A map for the interface of Bax oligomer was constructed based on the photocross-linking results (Fig. 6). A striking feature of this map is that most of the interface sites are located in or near the rear pocket on Bax (originally identified as the binding site for a stabilized Bim BH3 helix (31), see Fig. 1*A*), and in the helix 2, which shares a strong sequence and structural homology with the Bim BH3 helix (5, 31, 51). For example, residues 24, 47, 134, and 145 are located in the rear pocket, and residues 68, 69, and 73 are in the BH3 region that is part of the front pocket. Thus, this interface map seems in line with the one interface model in which a Bax oligomer is formed via a series of front:rear interfaces (Fig. 1*C*). Other sites involved in photocross-linking can be included in the interface, if it can be extended to include residue 79 in helix 3 and 82 in the loop 3 located near the front pocket, and 37 in the loop 1 located near the rear pocket. The expansion of the interface is conceivable considering that the Bax:Bax interface may have more contacts than the Bax:BH3 peptide interface. However, the photocross-linking data also can be explained by the two-interface model that includes the front:front and rear:rear interfaces (Fig. 1*B*).

Photocross-linking of Bax BH3 Peptide with Bax Protein Supports the Two-interface Model for Bax Oligomerization—To test which interface model is correct for the Bax oligomer, we used a peptide that contains both helices 2 and 3 (H2–H3) of Bax that could interact with either the front or the rear pocket depending on which model is correct. The peptide was cross-linked to [^{35}S]Met-Bax with ANB labeled at a single Lys either in the front or rear pocket (Fig. 7). A radioactive photoadduct that has a slightly higher molecular mass than [^{35}S]Met-Bax was detected when the photoreactive probe was located in the front pocket (K73 and K79) but not the rear pocket (K24, K37, K47, K134, and K147) (Fig. 7*A*, *lane 2*, indicated by *arrow*, Fig. 7*B*; data not shown for K73). This photoadduct is most likely formed by the peptide and the [^{35}S]Met-Bax, because it was not detected in the absence of the peptide (Fig. 7*A*, *lane 4*). Moreover, the photoadduct formed in the presence of a short peptide that only contains helix 2 (H2) had a lower apparent molecular mass than the one formed in the presence of the long H2–H3 peptide (Fig. 7*A*, *lane 6*, indicated by *arrow*). The yield of the photoadduct containing the short peptide is lower than the one containing the long peptide, indicating that the short peptide has lower affinity for Bax protein than the long one. This is consistent with our previous finding that the long peptide can activate Bax to permeabilize membranes more efficiently than the short one (32). Interestingly, the peptide with a Gly^{67} to Arg mutation that did not activate Bax in membranes also did not

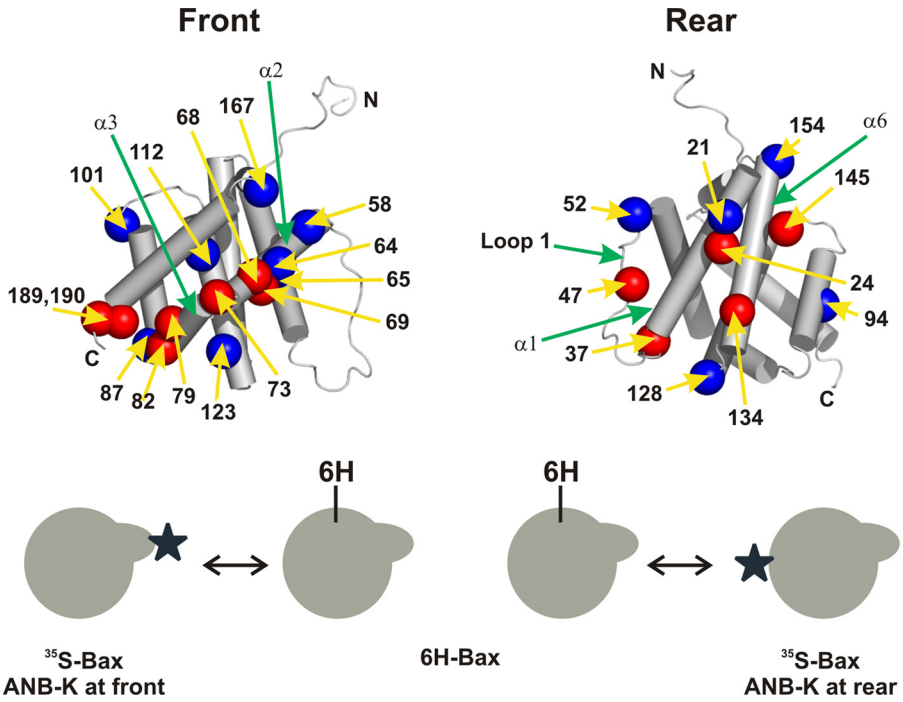

FIGURE 6. **Potential interface of Bax oligomerization.** Based on the site-specific photocross-linking data shown above, the surfaces of Bax that may form the oligomer interface were modeled on the previously determined Bax structure (5). The residues that resulted in Bax dimer-specific photoadduct when replaced by ANB-Lys and hence were close to or within the interface are in *red*, whereas the residues that did not result in the photoadduct and hence were likely far from the interface are in *blue*. The radii of these residues are increased to 6 Å to reflect the uncertainty of the photocross-linking-based mapping technique (36). The position of these residues in the Bax sequence is indicated by *number*. The *view* on the *left* and *right* shows the front pocket and rear pocket, respectively. The *schematic* underneath each *view* illustrates that the Bax protein with ANB-Lys at either the front or rear pocket interacts with the His_6-tagged Bax.

cross-link to the Bax with the photoreactive probe labeled at the front pocket (Fig. 7*A*, lanes 5 and 7), supporting that the peptide-protein interaction detected in the photocross-linking reaction is functionally relevant.

Since the H2–H3 peptide is part of the front pocket of Bax protein, cross-linking of it to the sites located in the front pocket of Bax protein supports the two interface model in which one of the interfaces is formed by the front pockets from two adjacent Bax proteins (Fig. 1*B*). In contrast, the cross-linking experiments did not reveal the front:rear interaction predicted by the one interface model (Fig. 1*C*).

Interaction at the Front Pocket of Bax Alters the Interaction at Its Rear Pocket—In the cross-linking reaction containing [^{35}S]Met-Bax with the photoreactive probe labeled at K134 or K145, there was a photoadduct formed in the presence of the mutant H2–H3 peptide (Fig. 7*B*, *lane 8* or *10*, respectively, indicated by the *arrowhead*). This adduct was most likely resulted from cross-linking of [^{35}S]Met-Bax with a reticulocyte protein in the *in vitro* translation system. It was noted that the adduct was not formed in the presence of the wild-type H2–H3 peptide (Fig. 7*B*, *lanes 7* and *9*). Because the wild-type peptide interacts with [^{35}S]Met-Bax, but the mutant does not (Fig. 7*A*), only the authentic peptide interaction with Bax inhibits the Bax interaction with the reticulocyte protein. The cross-linking of the reticulocyte protein with Bax was only detected when the photoreactive probe is labeled at K134 and K145, but not other lysines. Therefore, the reticulocyte protein most likely interacts with the rear pocket where the K134 and K145 are located. Because the peptide interacts with Bax at the front pocket, the interaction of the peptide with Bax at the front pocket inhibits the interaction of the reticulocyte protein with Bax at the rear pocket. The interaction at the front pocket thus likely alters the conformation of the rear pocket releasing the reticulocyte protein. Intriguingly the cross-linking of [^{35}S]Met-Bax with the reticulocyte protein was also inhibited in the presence of His_6-Bax (Fig. 7*C*, compare *lanes 1* with *3*, and *4* with *6*, indicated by *arrowhead*), suggesting that binding of His_6-Bax to the front pocket of [^{35}S]Met-Bax may release the reticulocyte protein from the rear pocket, thereby exposing the rear pocket for binding of other His_6-Bax resulting in the [^{35}S]Met-Bax:His_6-Bax photoadduct (Fig. 7*C*, *lanes 1* and *4*, indicated by *arrow*). Taken together these data suggest that the interaction at the front pocket primes the rear pocket for interaction.

To examine this hypothesis in a different way we introduced a G67R mutation into the front pocket of Bax. This mutation, when introduced into both [^{35}S]Met- and His_6-Bax proteins, greatly inhibited the interaction between the two proteins, because much less [^{35}S]Met-Bax coprecipitated with Ni^{2+}-bound His_6-Bax-G67R than His_6-Bax (Fig. 8*A*, *top image*, compare the *open circle*-indicated [^{35}S]Met-Bax bands in samples containing His_6-Bax-G67R or His_6-Bax with the control containing neither of these proteins). Equal amounts of [^{35}S]Met-Bax were used in the coprecipitation assay as indicated by the equivalent intensity of [^{35}S]Met-Bax bands in the *bottom image* of Fig. 8*A* (indicated by *open circle*). As expected, the cross-linking of His_6-Bax to [^{35}S]Met-Bax through the photoreactive probe attached to K79 in the front pocket of [^{35}S]Met-Bax was abolished when both proteins contained the G67R mutation (Fig. 8*A*, *top image*, *lane 8*, indicated by *arrow*). When compared with the cross-linking observed between the two proteins without the G67R mutation (Fig. 5, K79, *lane 2*) the cross-linking was not inhibited when the mutation was only in one of the proteins (*e.g.* [^{35}S]Met/ANB-Bax-K79-G67R) (Fig. 8*A*, *top image*, *lane 9*, indicated by *arrow*; data not shown for cross-linking of [^{35}S]Met/ANB-Bax K79 to His_6-Bax-G67R). These results can be interpreted by a model in which the front:front interface is symmetric. As illustrated in Fig. 8*B*, the G67R mutation in the front pocket of one binding partner cannot disrupt the entire interface and hence the interaction (*middle diagram*), whereas the mutation in both binding partners abolishes the interaction (*bottom diagram*).

Surprisingly the G67R mutation in the front pocket also greatly reduced the cross-linking through the probe attached to

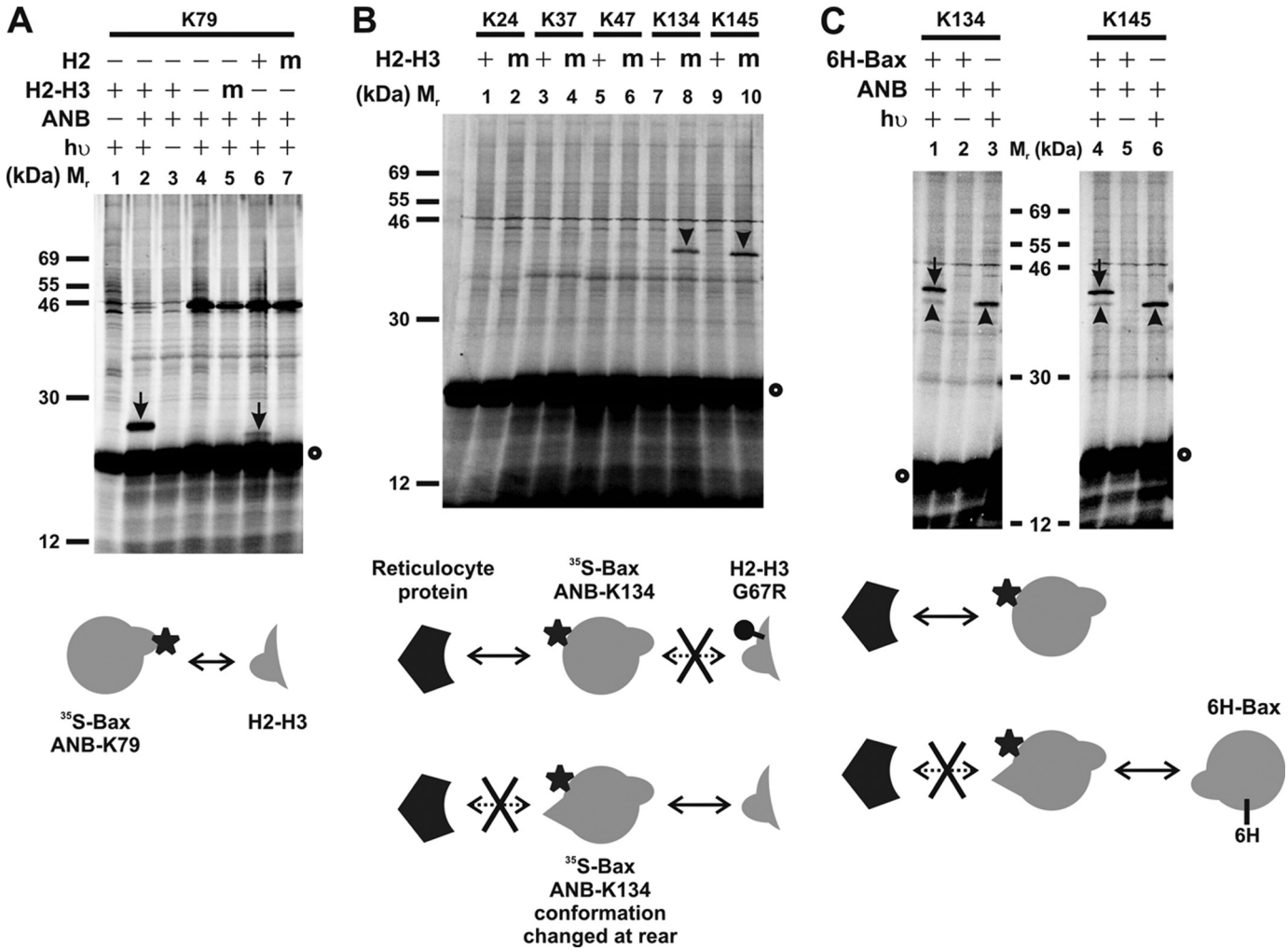

FIGURE 7. **Photocross-linking of Bax peptide to [^{35}S]Met- and ANB-labeled Bax protein.** *A*, total samples from cross-linking of [^{35}S]Met-Bax protein via the ANB probe attached to K79 in the front pocket with wild-type Bax peptide (H2 or H2–H3) or the corresponding G67R mutant peptide (*m*) were analyzed by SDS-PAGE and phosphorimaging. The *schematic* underneath illustrates the interaction between the Bax protein and peptide (*e.g.* H2–H3). The photoadduct containing [^{35}S]Met-Bax and H2–H3 or H2 is indicated by an *arrow* in *lane 2* or *6*, respectively. The photoadducts are specific to the corresponding protein-peptide complex, because they were not detected when ϵANB-Lys-tRNA^{Lys}, UV irradiation, or the peptide was omitted (*lanes 1*, *3*, or *4*; data not shown for H2), and when the mutant peptide was used (*lanes 5* or *7*). The [^{35}S]Met-Bax monomer is indicated by an *open circle*. *B*, total samples from cross-linking of [^{35}S]Met-Bax via the ANB attached to a single lysine located in the rear pocket with wild-type or mutant H2–H3 peptide were analyzed as above. The position of the single lysine is indicated at the *top*. The photoadduct between [^{35}S]Met-Bax with the ANB-K134 or -K145 and a reticulocyte protein, indicated by an *arrowhead* in *lane 8* or *10*, respectively, was detected in the presence of G67R mutant but not wild-type H2–H3 peptide. The *schematic* underneath illustrates that the wild-type peptide interacts with [^{35}S]Met/ANB-Bax at the front pocket, thus altering the rear pocket to release the reticulocyte protein (*bottom diagram*), whereas the mutant peptide does not have such activity, because it does not interact with Bax (*top diagram*). The *double-headed dashed arrow* with the *cross* indicates loss of interaction. *C*, total samples from cross-linking of [^{35}S]Met-Bax via the ANB-K134 or -K145 located in the rear pocket with His_6-Bax were analyzed as above, and their photoadduct, indicated by the *arrow* in *lane 1* or *4*, respectively, was confirmed by analyzing the corresponding Ni^{2+}-bound samples as shown in Fig. 5. The *arrowhead* indicates the photoadduct formed by the [^{35}S]Met/ANB-Bax protein and the reticulocyte protein that displays a lower apparent molecular mass compared with the photoadduct formed by [^{35}S]Met/ANB-Bax and His_6-Bax, likely because the reticulocyte protein has a lower molecular mass than His_6-Bax. The *schematic* underneath illustrates that the His_6-Bax interacts with [^{35}S]Met/ANB-Bax at the front pocket, thus altering the rear pocket to release the reticulocyte protein. Other *symbols* are as described in *panels A* and *B*.

K134 in the rear pocket (Fig. 8*A*, *top image*, compare the *arrowhead*-indicated bands in *lanes 2* and *3*), and this inhibitory effect was only observed when the mutation was introduced into both Bax proteins in the cross-linking reaction. Therefore, when the front-pocket mutation disrupted the front:front interface, it also disrupted the rear:rear interface (illustrated in Fig. 8*C*, *bottom diagram*), suggesting that binding at the rear pocket is dependent on the binding at the front pocket. The binding at the front pocket may induce a conformational change at the rear pocket (Fig. 8*C*, *top diagram*), as suggested by the fact that binding of Bax peptide or protein to the front pocket inhibited binding of the reticulocyte protein to the rear pocket (Fig. 7). We therefore concluded that binding of two Bax proteins through the front pockets primes the rear pockets for binding of other Bax proteins (illustrated in the *top diagram* of Fig. 8*C*, the two proteins on the *left* as well as the two on the *right* bind through the front pocket first, then the two resulting dimers bind through the conformation changed rear pocket to form a tetramer).

DISCUSSION

We have used site-specific photocross-linking to systematically map the interface of Bax oligomer. By combining the results from this and previous studies (22, 25, 28, 31–32), it is

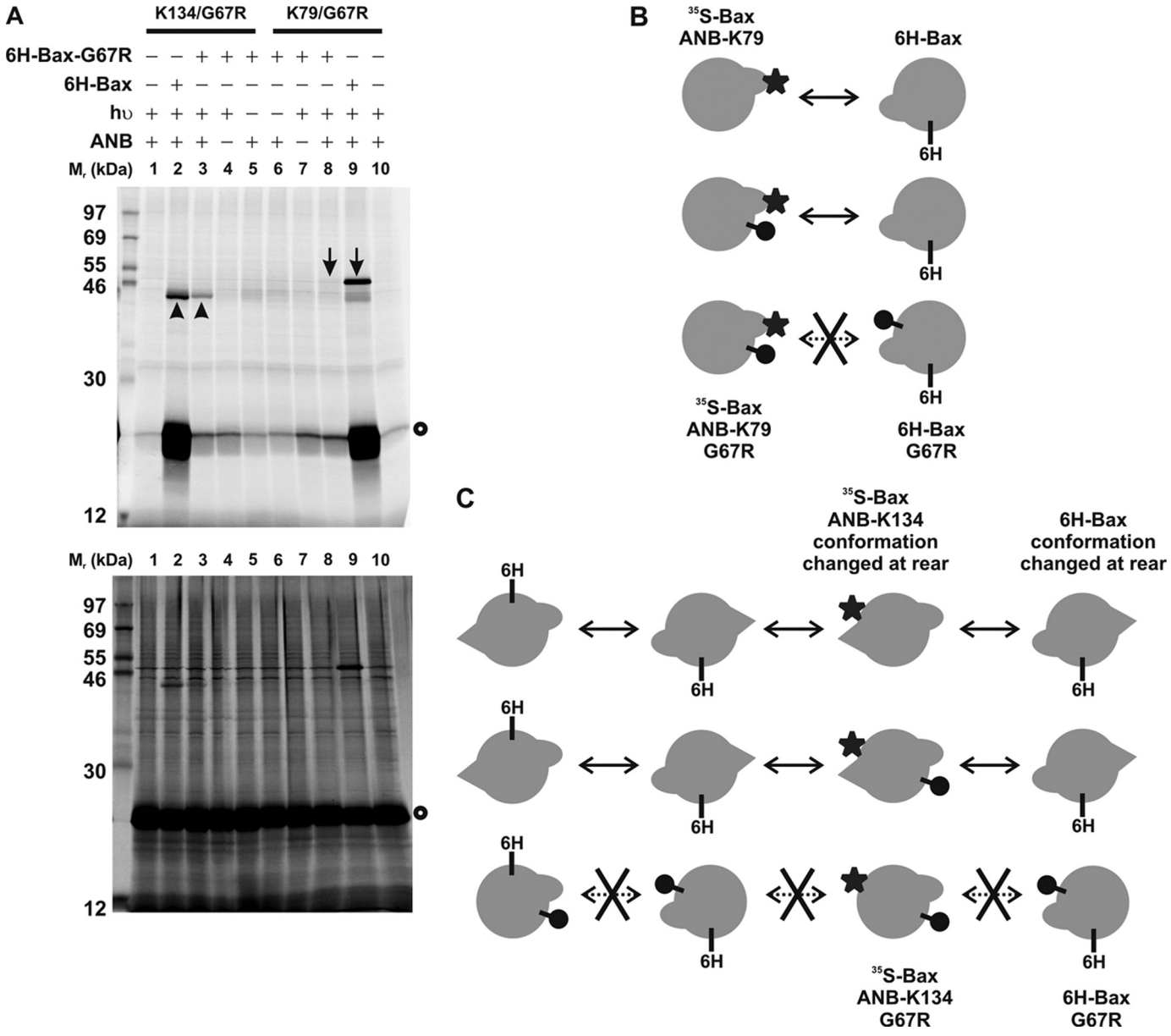

FIGURE 8. **Effect of a mutation in the front pocket on cross-linking of His_6-Bax to [^{35}S]Met-Bax via photoprobe attached to the front or rear pocket.** *A*, [^{35}S]Met-labeled Bax-G67R with ANB attached to either K79 in the front pocket or K134 in the rear pocket was cross-linked to either His_6-Bax or the G67R mutant and analyzed as above. The phosphor images from the total photolyzed and Ni^{2+}-bound samples are shown at the *bottom* and *top*, respectively. The *arrow* and *arrowhead* in *lanes 9* and *2* indicate the photoadduct resulted from cross-linking of [^{35}S]Met/ANB-Bax-G67R-K79 and -K134 to His_6-Bax, respectively. Formation of both photoadducts was diminished by the G67R mutation in His_6-Bax (*lanes 8* and *3*). The two photoadducts display slightly different migrations on the gel, because they were formed by cross-linking through photoprobes attached to different sites in [^{35}S]Met-Bax that would react with different residues in His_6-Bax. The *open circle* indicates the monomer of [^{35}S]Met-labeled Bax proteins. *B*, *schematic* illustration of the interaction between [^{35}S]Met-Bax with ANB in the front pocket (*e.g.* ANB-K79) and His_6-Bax through the front:front interface, and the effect of G67R mutation in the front pocket on the interaction. The data for the interaction between wild-type [^{35}S]Met/ANB-Bax-K79 and His_6-Bax are shown in Fig. 5. *C*, *schematic* illustration for how the conformation and interaction at the rear pocket was altered by interaction at the front pocket, and how the conformation and interaction were affected by the front pocket mutation.

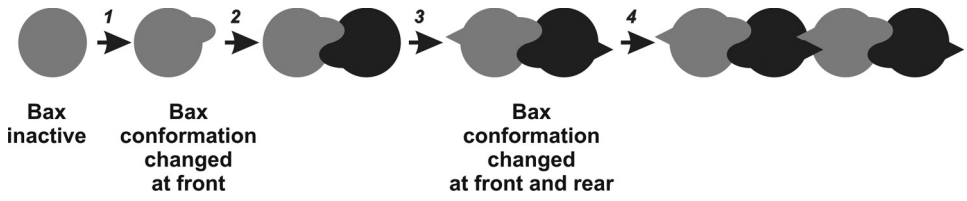

FIGURE 9. **A stepwise model for Bax oligomerization.** Bax oligomerization may occur through the following steps. *1*, upon activation, Bax changes conformation to expose the front pocket; *2*, the conformation-altered Bax dimerizes through interaction at the front pocket; *3*, the interaction at the front pocket alters the conformation at the rear pocket; and *4*, two Bax dimers with the altered rear pocket bind and form a tetramer that can grow into larger oligomers by adding more similar Bax dimers at the rear pocket ends. Neighboring Bax molecules in the dimer and tetramer are *shaded differently* for clarity, although they have the same conformation and interaction.

possible to model how active Bax can form an oligomer and how Bcl-2 can inhibit Bax oligomerization.

Implications for Bax Activation and Oligomerization—The salient feature of our model is that each protein in the oligomer contributes two surfaces to interact with neighboring proteins (Fig. 9). Although a single exposed surface is sufficient to form dimers, both surfaces need

to be exposed before oligomerization can take place. Soluble Bax monomers are most likely in a conformation with the BH1–3 groove occluded by α9 but the rear pocket exposed (the substrate before *step 1* in Fig. 9) (5). A BH3-only protein may bind the rear pocket of Bax using their BH3 motif as suggested previously (22, 28, 31). The binding may change Bax conformation releasing α9 from the BH1–3 groove such that the hydrophobic α9 can insert into membrane (Fig. 9, *step 1*). Dislodging of α9 would expose and alter the BH1–3 groove to form the front pocket that in turn could bind the front pocket of another Bax, which has been similarly activated by a BH3-only protein (*step 2*). Alternatively or additionally, the first activated Bax may use its exposed BH3 region to bind the rear pocket of a soluble Bax monomer. This binding would activate the Bax monomer in the same way as the binding of BH3-only protein does. In this way the initial activation of Bax by BH3-only protein can be amplified through Bax auto-activation as we observed before (32). No matter how Bax proteins are activated, some of them will have the front pocket exposed. These pockets can engage with each other to form the first Bax:Bax interface via the front:front interaction demonstrated in the current cross-linking study generating a dimer (Fig. 9, *step 2*). The formation of the front:front interface may alter the rear pocket of the two Bax proteins thereby releasing the activator, either a BH3-only or a Bax protein, from the pocket (*step 3*), a possibility that is consistent with the data that interaction of Bax BH3 peptide at the front pocket of a Bax protein releases the reticulocyte protein from the rear pocket of the Bax protein (Fig. 7). The interaction via the re-exposed but altered rear pocket of two Bax dimers generates a Bax tetramer (*step 4*). The tetramer can propagate into a larger oligomer by interaction with other dimers that are generated through the *steps 1–3*. Interestingly Bak, a structural homolog of Bax, was shown to form oligomers with two similar interfaces in recent studies (14, 15). These studies also show that the front:front interface is symmetric and formation of the rear:rear interface depends on the interaction at the front:front interface. Therefore, despite their difference in terms of intracellular location and interaction prior to activation, Bax and Bak may form similar oligomers via similar mechanisms after activation, consistent with their functional redundancy.

We noted that G67R mutation was recently suggested to inhibit the tBid-induced conformational change that is required for Bax oligomerization (28). This could provide an alternative interpretation of our cross-linking data with the mutant. However, our interpretation is supported by the fact that the G67R Bax mutant still cross-linked with a wild-type Bax, therefore, the mutant should be in an oligomerization competent conformation. The difference between our and their observations is most likely that the mutant protein can still be activated by detergent. In fact even tBid can partially activate Bax resulting in oligomer formation as detected in their gel-filtration assay, suggesting that the mutant retains some potential to be activated and form oligomers.

The Bax oligomer may grow while each protein in the oligomer is in the tail-anchoring conformation with the α9 helix inserted into the membrane and the rest of the protein retained on the membrane surface similar to the locale suggested for Bak (52). The interaction between the α9 sequences may occur at this stage as suggested by our cross-linking data from the photoreactive probe attached to the C-terminal end of α9 (Fig. 5, K189,190). The tail-anchored oligomer may switch to the multispanning conformation with additional sequences, such as α5 and α6, inserted into the membrane. This conformational switch may occur after the oligomer reaches a certain size, and may lead to permeabilization of the membrane. However, such a mechanism completely disagrees with our previous study in which monomers of activated Bax with α5, α6, and α9 embedded in the membrane were found in the absence of oligomerization (27). Therefore, the conformational change caused by binding of BH3-only protein to the rear pocket of soluble or peripheral membrane-bound Bax may induce a transition from the cytoplasmic to the multispanning state. The BH3 region in the multispanning Bax may be exposed on the membrane surface to engage other soluble/peripheral Bax molecules inducing the same conformational transition. In this alternative model, the Bax oligomer grows as each monomer switches to the multispanning conformation. The membrane permeabilization may start when the multispanning Bax oligomer grows to certain size. The extent of permeabilization or the pore size may increase thereafter as more multispanning monomers are added to the oligomer. Because there is no evidence for a maximal Bax pore size, there may be no constraints on the eventual size of the oligomer. The cross-linking approaches that we and others have used will help us to map the interface for the pore-forming oligomer (14, 36).

Implications for How Bcl-2 Inhibits Bax Activation and Oligomerization—Bcl-2 can bind to BH3-only proteins preventing them from activating Bax. Bcl-2 can also sequester the activated Bax proteins inhibiting their conformational change and oligomerization (1, 18). Thus, Bcl-2 may bind to the exposed BH3 region in the activated Bax to prevent it from activating other Bax molecules through auto-activation (32) and from oligomerizing with other activated Bax (44). In addition, it is also possible that Bcl-2 may bind to the rear pocket of the Bax dimer to prevent it from forming the tetramer. Our preliminary cross-linking data suggest that both types of Bcl-2-Bax interaction exist. Further experiments are underway to determine the extent of overlap between the Bax:Bcl-2 and Bax:Bax interfaces.

Triton X-100 Induces Bax Oligomerization Accompanied by Conformational Change—We used Triton X-100 to induce Bax oligomerization that likely occurs after or concomitantly with the conformational change induced by the detergent. Triton X-100 exposes an N-terminal epitope between residues 13 and 19 that is recognized by 6A7 monoclonal antibody (8, 53). This epitope is buried in the soluble Bax in healthy cells (8) and becomes exposed upon apoptotic stimuli when the Bax is bound to the mitochondrial membrane (26, 28, 54). In solution the 6A7 epitope can be reversibly exposed by liposomes (37). Addition of tBid to the Bax/liposome mixture makes the epitope exposure irreversible, which accompanies Bax oligomerization in the liposomal membrane. Interestingly the 6A7 epitope is buried in the hetero-complex formed between Bax and Bcl-2 or Bcl-x_L in Triton X-100 (8, 40). Because this epitope overlaps with the helix 1, which is part of the rear pocket of Bax

(see Fig. 1*A*), Bcl-2 or Bcl-xL may bind to this pocket and mask the epitope. Together these observations suggest that the conformational change of Bax induced by Triton X-100 shares some characteristics with the conformational change induced by apoptotic stimuli.

Numerous studies have shown that Bax oligomerizes in various detergents, including Triton-X-100, similarly to the membrane-embedded Bax (18, 40, 42, 44). Bax oligomers formed in detergents or membranes can be detected by gel-filtration chromatography and chemical cross-linking. It is therefore surprising that Bax was found as a monomer in the micelles of several detergents, including Triton X-100, in a recent study (34). This study used a fluorescent Bax mutant lacking α9 and fluorescence correlation spectroscopy and fluorescence-intensity distribution analysis. The results from our photocross-linking study are not in accord with the above conclusion. In particular, photoadducts of Bax dimer were detected in Triton X-100 micelles when the photoreactive probe was located at multiple sites on the Bax protein, demonstrating that the Bax proteins in the micelle are in close proximity, which strongly suggests a direct molecular interaction. The reason for the difference in conclusions is likely that we used full-length Bax protein, whereas Ivashyna *et al.* used truncated protein without the C-terminal α9. Consistent with this possibility we have shown that the C terminus is involved in the Bax:Bax interaction by cross-linking through a C-terminal photoreactive probe (Fig. 5, K189,190).

In summary, our site-specific photocross-linking study provides the first comprehensive interface map of the Bax oligomer that is formed in detergent micelles. Our system mimics apoptotic stimuli to activate Bax monomers and native membranes to let the activated Bax form oligomer. Our data support a two-interface model in which Bax oligomerizes through two separated interfaces, and formation of one interface depends on formation of the other interface. Furthermore, Bax activation and oligomerization likely progress through a sequence of steps, each of which may be targeted for therapeutic gains to treat apoptosis-related diseases.

Acknowledgment—We thank Gillian Air for thoroughly editing the manuscript.

REFERENCES

1. Leber, B., Lin, J., and Andrews, D. W. (2007) *Apoptosis* **12,** 897–911
2. Youle, R. J., and Strasser, A. (2008) *Nat. Rev. Mol. Cell Biol.* **9,** 47–59
3. Lalier, L., Cartron, P. F., Juin, P., Nedelkina, S., Manon, S., Bechinger, B., and Vallette, F. M. (2007) *Apoptosis* **12,** 887–896
4. Kvansakul, M., Yang, H., Fairlie, W. D., Czabotar, P. E., Fischer, S. F., Perugini, M. A., Huang, D. C., and Colman, P. M. (2008) *Cell Death Differ.* **15,** 1564–1571
5. Suzuki, M., Youle, R. J., and Tjandra, N. (2000) *Cell* **103,** 645–654
6. Moldoveanu, T., Liu, Q., Tocilj, A., Watson, M., Shore, G., and Gehring, K. (2006) *Mol. Cell* **24,** 677–688
7. Wolter, K. G., Hsu, Y. T., Smith, C. L., Nechushtan, A., Xi, X. G., and Youle, R. J. (1997) *J. Cell Biol.* **139,** 1281–1292
8. Hsu, Y. T., and Youle, R. J. (1998) *J. Biol. Chem.* **273,** 10777–10783
9. Wei, M. C., Lindsten, T., Mootha, V. K., Weiler, S., Gross, A., Ashiya, M., Thompson, C. B., and Korsmeyer, S. J. (2000) *Genes Dev.* **14,** 2060–2071
10. Pagliari, L. J., Kuwana, T., Bonzon, C., Newmeyer, D. D., Tu, S., Beere, H. M., and Green, D. R. (2005) *Proc. Natl. Acad. Sci. U.S.A.* **102,** 17975–17980
11. Schinzel, A., Kaufmann, T., Schuler, M., Martinalbo, J., Grubb, D., and Borner, C. (2004) *J. Cell Biol.* **164,** 1021–1032
12. Wei, M. C., Zong, W. X., Cheng, E. H., Lindsten, T., Panoutsakopoulou, V., Ross, A. J., Roth, K. A., MacGregor, G. R., Thompson, C. B., and Korsmeyer, S. J. (2001) *Science* **292,** 727–730
13. Eskes, R., Desagher, S., Antonsson, B., and Martinou, J. C. (2000) *Mol. Cell. Biol.* **20,** 929–935
14. Dewson, G., Kratina, T., Sim, H. W., Puthalakath, H., Adams, J. M., Colman, P. M., and Kluck, R. M. (2008) *Mol. Cell* **30,** 369–380
15. Dewson, G., Kratina, T., Czabotar, P., Day, C. L., Adams, J. M., and Kluck, R. M. (2009) *Mol. Cell* **36,** 696–703
16. Willis, S. N., Chen, L., Dewson, G., Wei, A., Naik, E., Fletcher, J. I., Adams, J. M., and Huang, D. C. (2005) *Genes Dev.* **19,** 1294–1305
17. Cheng, E. H., Sheiko, T. V., Fisher, J. K., Craigen, W. J., and Korsmeyer, S. J. (2003) *Science* **301,** 513–517
18. Billen, L. P., Kokoski, C. L., Lovell, J. F., Leber, B., and Andrews, D. W. (2008) *PLoS Biol.* **6,** e147
19. Sattler, M., Liang, H., Nettesheim, D., Meadows, R. P., Harlan, J. E., Eberstadt, M., Yoon, H. S., Shuker, S. B., Chang, B. S., Minn, A. J., Thompson, C. B., and Fesik, S. W. (1997) *Science* **275,** 983–986
20. Willis, S. N., Fletcher, J. I., Kaufmann, T., van Delft, M. F., Chen, L., Czabotar, P. E., Ierino, H., Lee, E. F., Fairlie, W. D., Bouillet, P., Strasser, A., Kluck, R. M., Adams, J. M., and Huang, D. C. (2007) *Science* **315,** 856–859
21. Mérino, D., Giam, M., Hughes, P. D., Siggs, O. M., Heger, K., O'Reilly, L. A., Adams, J. M., Strasser, A., Lee, E. F., Fairlie, W. D., and Bouillet, P. (2009) *J. Cell Biol.* **186,** 355–362
22. Cartron, P. F., Gallenne, T., Bougras, G., Gautier, F., Manero, F., Vusio, P., Meflah, K., Vallette, F. M., and Juin, P. (2004) *Mol. Cell* **16,** 807–818
23. Cartron, P. F., Arokium, H., Oliver, L., Meflah, K., Manon, S., and Vallette, F. M. (2005) *J. Biol. Chem.* **280,** 10587–10598
24. Desagher, S., Osen-Sand, A., Nichols, A., Eskes, R., Montessuit, S., Lauper, S., Maundrell, K., Antonsson, B., and Martinou, J. C. (1999) *J. Cell Biol.* **144,** 891–901
25. Lovell, J. F., Billen, L. P., Bindner, S., Shamas-Din, A., Fradin, C., Leber, B., and Andrews, D. W. (2008) *Cell* **135,** 1074–1084
26. Nechushtan, A., Smith, C. L., Hsu, Y. T., and Youle, R. J. (1999) *EMBO J.* **18,** 2330–2341
27. Annis, M. G., Soucie, E. L., Dlugosz, P. J., Cruz-Aguado, J. A., Penn, L. Z., Leber, B., and Andrews, D. W. (2005) *EMBO J.* **24,** 2096–2103
28. Kim, H., Tu, H. C., Ren, D., Takeuchi, O., Jeffers, J. R., Zambetti, G. P., Hsieh, J. J., and Cheng, E. H. (2009) *Mol. Cell* **36,** 487–499
29. Letai, A., Bassik, M. C., Walensky, L. D., Sorcinelli, M. D., Weiler, S., and Korsmeyer, S. J. (2002) *Cancer Cell* **2,** 183–192
30. Chipuk, J. E., Fisher, J. C., Dillon, C. P., Kriwacki, R. W., Kuwana, T., and Green, D. R. (2008) *Proc. Natl. Acad. Sci. U.S.A.* **105,** 20327–20332
31. Gavathiotis, E., Suzuki, M., Davis, M. L., Pitter, K., Bird, G. H., Katz, S. G., Tu, H. C., Kim, H., Cheng, E. H., Tjandra, N., and Walensky, L. D. (2008) *Nature* **455,** 1076–1081
32. Tan, C., Dlugosz, P. J., Peng, J., Zhang, Z., Lapolla, S. M., Plafker, S. M., Andrews, D. W., and Lin, J. (2006) *J. Biol. Chem.* **281,** 14764–14775
33. Ruffolo, S. C., and Shore, G. C. (2003) *J. Biol. Chem.* **278,** 25039–25045
34. Ivashyna, O., García-Sáez, A. J., Ries, J., Christenson, E. T., Schwille, P., and Schlesinger, P. H. (2009) *J. Biol. Chem.* **284,** 23935–23946
35. Ho, S. N., Hunt, H. D., Horton, R. M., Pullen, J. K., and Pease, L. R. (1989) *Gene* **77,** 51–59
36. Zhang, Z., Lapolla, S. M., Annis, M. G., Truscott, M., Roberts, G. J., Miao, Y., Shao, Y., Tan, C., Peng, J., Johnson, A. E., Zhang, X. C., Andrews, D. W., and Lin, J. (2004) *J. Biol. Chem.* **279,** 43920–43928
37. Yethon, J. A., Epand, R. F., Leber, B., Epand, R. M., and Andrews, D. W. (2003) *J. Biol. Chem.* **278,** 48935–48941
38. Lin, J., Liang, Z., Zhang, Z., and Li, G. (2001) *J. Biol. Chem.* **276,** 41733–41741
39. Hjelmeland, L. M. (1990) *Methods Enzymol.* **182,** 277–282
40. Hsu, Y. T., and Youle, R. J. (1997) *J. Biol. Chem.* **272,** 13829–13834
41. Antonsson, B., Montessuit, S., Lauper, S., Eskes, R., and Martinou, J. C. (2000) *Biochem. J.* **345,** 271–278
42. Antonsson, B., Montessuit, S., Sanchez, B., and Martinou, J. C. (2001) *J. Biol. Chem.* **276,** 11615–11623

43. Bhairi, S. M. (2001) *Detergents: A Guide to the Properties and Uses of Detergents in Biological Systems*, pp. 37–41, Calbiochem-Novabiochem Corp., La Jolla, CA
44. Dlugosz, P. J., Billen, L. P., Annis, M. G., Zhu, W., Zhang, Z., Lin, J., Leber, B., and Andrews, D. W. (2006) *EMBO J.* **25,** 2287–2296
45. Yin, X. M., Oltvai, Z. N., and Korsmeyer, S. J. (1994) *Nature* **369,** 321–323
46. Krieg, U. C., Walter, P., and Johnson, A. E. (1986) *Proc. Natl. Acad. Sci. U.S.A.* **83,** 8604–8608
47. Zha, H., Aimé-Sempé, C., Sato, T., and Reed, J. C. (1996) *J. Biol. Chem.* **271,** 7440–7444
48. Wang, K., Gross, A., Waksman, G., and Korsmeyer, S. J. (1998) *Mol. Cell. Biol.* **18,** 6083–6089
49. Kim, H., Rafiuddin-Shah, M., Tu, H. C., Jeffers, J. R., Zambetti, G. P., Hsieh, J. J., and Cheng, E. H. (2006) *Nat. Cell Biol.* **8,** 1348–1358
50. Oltvai, Z. N., Milliman, C. L., and Korsmeyer, S. J. (1993) *Cell* **74,** 609–619
51. Liu, X., Dai, S., Zhu, Y., Marrack, P., and Kappler, J. W. (2003) *Immunity* **19,** 341–352
52. Dewson, G., and Kluck, R. M. (2009) *J. Cell Sci.* **122,** 2801–2808
53. Peyerl, F. W., Dai, S., Murphy, G. A., Crawford, F., White, J., Marrack, P., and Kappler, J. W. (2007) *Cell Death Differ.* **14,** 447–452
54. Makin, G. W., Corfe, B. M., Griffiths, G. J., Thistlethwaite, A., Hickman, J. A., and Dive, C. (2001) *EMBO J.* **20,** 6306–6315

Bax Forms an Oligomer via Separate, Yet Interdependent, Surfaces

Zhi Zhang, Weijia Zhu, Suzanne M. Lapolla, Yiwei Miao, Yuanlong Shao, Mina Falcone, Doug Boreham, Nicole McFarlane, Jingzhen Ding, Arthur E. Johnson, Xuejun C. Zhang, David W. Andrews and Jialing Lin

J. Biol. Chem. 2010, 285:17614-17627.
doi: 10.1074/jbc.M110.113456 originally published online April 9, 2010
